A New Algorithm for the Wide-Band Analysis of Arbitrarily Shaped Planar Circuits

PAOLO ARCIONI, MARCO BRESSAN AND GIUSEPPE CONCIAURO, MEMBER, IEEE

Abstract — **A new algorithm for the wide-band analysis of the two-dimensional model of a planar circuit is described. The planar circuit is considered to be enclosed in a regularly shaped (rectangular or circular) resonator, and the electric and magnetic fields are derived from the Green's functions of this resonator by integrating over the periphery of the circuit not coinciding with the regular shape. The special form used for the Green's functions makes it possible to derive the Z parameters in a special form, similar to Foster's series, but converging much more rapidly. The calculation requires the determination of a reduced number of resonances of the planar circuit, which are obtained by an integral equation approach leading to a linear eigenvalue problem. The algorithm was implemented in an efficient CAD routine, named ANAPLAN, which is briefly described.**

I. INTRODUCTION

IN COMPARISON with usual line elements, strip and microstrip planar elements allow a greater flexibility in MIC and MMIC design. The possibility of considering a virtually infinite variety of shapes may lead to interesting solutions in the design of many circuit components, such as directional couplers, filters, and chokes. Since the publication of the early papers on planar circuits [1]–[4], interest in this subject has increased continuously. An extensive bibliography on both methodological and applicative aspects can be found in [5] and in a recent survey paper by Sorrentino [6].

The design flexibility inherent in planar circuit philosophy can be fully exploited only if CAD tools suitable for the wide-band analysis and optimization of arbitrary shapes are available. Fast algorithms for analysis are of paramount importance, as trial-and-error optimum design techniques require a significant number of sequential analyses.

A simple model used in the analysis of planar circuits assumes that the circuit is laterally bounded by a magnetic wall, except at the ports (Fig. 1(a)). Since in this model the (z-directed) electric field and the (transversal) magnetic field are z-independent, the field analysis is two-dimensional and it is much simpler than the three-dimensional one which would be required for taking into account fringing field and radiation effects rigorously. The use of this model is well established in the analysis of strip (triplate) planar circuits, where the fringing field effects are taken into account by a slight enlargement of the transversal circuit dimensions [5]. The same model was used for the analysis of microstrip planar resonators [7], [8] and circuits [9], [10]. In these last cases the fringing field effect was taken into account by considering an enlarged circuit pattern and an effective permittivity. Though the two-dimensional model is less accurate in microstrip than in triplate circuit analysis, it is, however, a useful starting point in the design of such circuits.

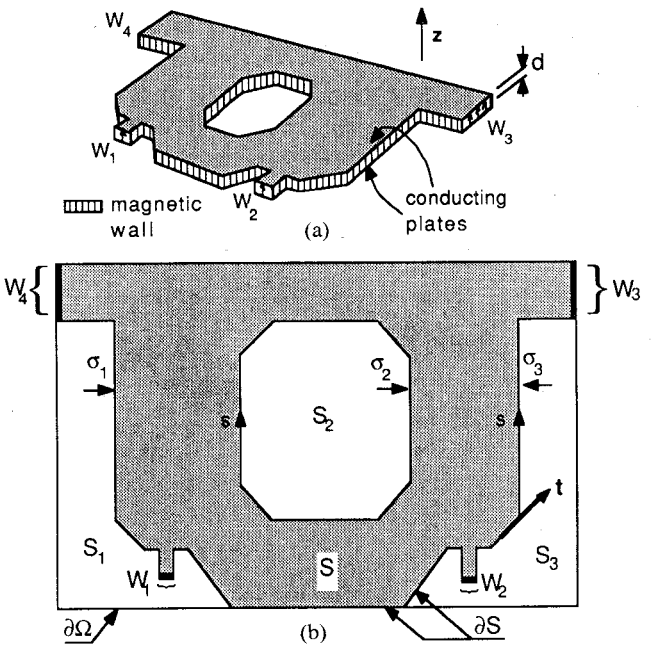

Fig. 1. (a) Two-dimensional model of a planar circuit. (b) Planar circuit enclosed inside a rectangular resonator Ω. In this example $\Omega = S + S_1 + S_2 + S_3$; $\sigma = \sigma_1 + \sigma_2 + \sigma_3$.

Thus far, three kinds of methods have been proposed for the analysis of planar elements of arbitrary shapes: i) the time-domain approach [11]; ii) the contour integral method [4]; and iii) the eigenfunction expansion method [12]. The time-domain approach has the advantage of permitting the analysis of circuits including nonlinear elements, but it leads to computer times that are prohibitive for CAD applications. The contour integral method is very efficient for single-frequency calculations, but it may require a very

Manuscript received April 15, 1987; revised December 12, 1987, and May 18, 1988. This work was supported by CNR, Progetto Finalizzato MADESS, under contract 86.02188.61.

The authors are with the Dipartimento di Elettronica, Università di Pavia, 27100 Pavia, Italy.

IEEE Log Number 8822911.

0018-9480/88/1000-1426$01.00 ©1988 IEEE

long frequency-by-frequency analysis when used in wide-band design.

In principle the eigenfunction expansion method is well suited for wide-band analyses, as it supplies directly the poles and the residues necessary to determine the Y parameters on the basis of their Foster representation. This method requires the determination of the resonating modes of the circuit when the ports are shorted, since each pair of poles is given by the resonating frequency of a mode and the pertinent residues depend on the modal field. Due to the relatively slow convergence of the Foster series, in order to achieve a good accuracy in a wide band, the number of modes to be considered must be much larger than the number of modes occurring in the band of interest. This is a serious drawback, because the modes must be determined numerically using, for example, the finite element technique. For this reason, even though this method is the most suitable for wide-band analyses, its practical use requires a very long computer time.

In this paper we present a new algorithm, well suited for wide-band analyses of planar circuits of arbitrary shapes, represented by their two-dimensional model. The algorithm leads to the determination of all the unknown coefficients included in the following representation of the Z parameters:

$$Z_{ij}(k) = \frac{\eta d}{jkS} + jk\eta d\Lambda_{ij} + j\frac{k^3\eta}{d}\sum_{q=1}^{Q}\frac{V_{iq}V_{jq}}{k_q^2\left(k_q^2-k^2\right)} \qquad (i,j=1,\cdots,N). \quad (1)$$

In this expression N is the number of the ports, S is the area of the planar circuit (see Fig. 1(b)), d is the thickness of the dielectric, $\eta=\sqrt{\mu/\epsilon}$ and $k=\omega\sqrt{\epsilon\mu}$ are the characteristic impedance and the wavenumber, respectively, Λ_{ij} are real frequency-independent coefficients, and the quantities k_q are the first Q resonating wavenumbers of the circuit when its ports are open. The coefficients V_{iq} are related to the normalized electric field $E^{(q)}$ of the qth resonant mode by

$$V_{iq} = -\frac{d}{W_i}\int_{W_i} E^{(q)}\,ds \qquad (2)$$

where s is a coordinate taken along the boundary ∂S, and W_i denotes both the ith port and its width. The first term in (1) dominates at very low frequencies and represents the contribution of the parallel-plate capacitance.

Like the eigenfunction expansion method, our algorithm also involves the calculation of resonant modes. Their number, however, is strongly reduced because of the quite good convergence of the series contained in (1). In order to appreciate this point (1) should be compared with the usual Foster-type representation of the Z parameters, obtained by the Green's function approach [5]:

$$Z_{ij}(k) = \frac{\eta d}{jkS} + j\frac{\eta k}{d}\sum_{q=1}^{\infty}\frac{V_{iq}V_{jq}}{k_q^2-k^2}. \qquad (3)$$

It is realized that (1) represents a modification of (3), obtainable from it by adding and subtracting from the series its low-frequency approximation (corresponding to $d^2\Lambda_{ij}$) and by retaining in the remaining series the first Q terms. The extraction of $d^2\Lambda_{ij}$ improves the convergence of the series, due to the appearance of the factor k_q^2 in the denominator of its terms. Since our algorithm leads to the direct determination of the coefficients Λ_{ij} (i.e., independently of their series representation), the number of modes to be calculated is strongly reduced. In practice it does not much exceed the number of resonances occurring in the band of interest (see Section V).

The two basic equations of the theory are derived from the integral representation of the field in terms of its boundary value. In setting up these equations the planar circuit is considered as enclosed inside a two-dimensional circular or rectangular resonator Ω, bounded by a magnetic wall too (see Fig. 1(b)). This unusual configuration is considered in order to represent the field by integrals involving the Green's functions of the resonator Ω, which can be approximated very well by rational functions of k. This causes the basic equations to assume a particular form which makes it possible to deduce (1) and to set up the algorithm for the calculation of all the coefficients involved therein. It is noted that this particular form makes it possible to determine the resonating wavenumbers very efficiently by solving a linear eigenvalue problem, following a procedure similar to that employed by Conciauro *et al.* [13] for the determination of waveguide modes.

Since it is based on an integral equation approach, our method shares some of the merits of the contour integral method (in particular with regard to the relatively small order of the involved matrices), without the drawback of requiring a frequency-by-frequency analysis. Furthermore, in cases where a part of the boundary ∂S coincides with $\partial\Omega$ (as in the case of Fig. 1(b)), the boundary condition has to be imposed only on the other part, so that the number of variables involved in the solution of the equations and the order of the matrices may be reduced significantly.

It is worth noting that a similar algorithm can be developed for the analysis of planar waveguide circuits, the main difference being the electrical wall condition on the lateral bounary. Actually, in that case a physical reasoning makes it possible to derive the first two terms of (1) straightforwardly, with a significant simplification [14].

II. Basic Equations

Let $\boldsymbol{z}$ be the unit vector along the z axis and $\boldsymbol{t}=\boldsymbol{t}(s)$ the tangent unit vector along the boundary ∂S, and let $\boldsymbol{E}=\boldsymbol{z}E(s)$ denote the electric field thereat. Moreover let $I_1, I_2, \cdots, I_N$ be the currents impressed at the N ports, which are z-directed and uniformly distributed on sheets having widths W_i. Due to the equivalence theorem, the field inside the region S, may be considered as generated by an (unknown) equivalent magnetic current sheet $-\boldsymbol{t}E(s)$ flowing along ∂S and by the electric current sheet

$$\boldsymbol{z}\sum_{i=1}^{N}\frac{I_i}{W_i}u_i(s)$$

where $u_i(s)=1$ at the ith port and zero elsewhere. Note that the electric current is zero outside the ports due to the magnetic-wall condition at the boundary of the planar circuit.

Since the equivalence theorem establishes that the field produced by these currents is zero outside the region S, it is unimportant to consider them as radiating in free space or inside a cylindrical impedance wall $\partial\Omega$, bounding a region Ω which includes S (Fig. 1(b)). Therefore we are permitted to assume that the currents act inside an outer *rectangular* or *circular* two-dimensional resonator Ω bounded by a magnetic wall. One of the advantages of this assumption can be appreciated at this point: in fact, since it permits ∂S and $\partial\Omega$ to coincide partially (for particular shapes of S), the unknown magnetic current can be reduced to that flowing in the noncommon portion of the boundaries (magnetic currents backed by magnetic wall have no effect). In the following the portion of ∂S not coinciding with $\partial\Omega$ will be denoted by σ. It is understood that σ coincides with ∂S in cases where ∂S and $\partial\Omega$ have no common parts.

The field generated by the current sheets in the resonator Ω is given by

$$E(\boldsymbol{r}) = -j\eta k \sum_{i=1}^{N} \frac{I_i}{W_i} \int_{W_i} g_{11}(\boldsymbol{r},\boldsymbol{r}',k)\,ds' + \int_{\sigma} \boldsymbol{g}_{12}(\boldsymbol{r},\boldsymbol{r}',k)\cdot \boldsymbol{t}' E(s')\,ds' \tag{4a}$$

$$\boldsymbol{H}(\boldsymbol{r}) = -\sum_{i=1}^{N} \frac{I_i}{W_i} \int_{W_i} \boldsymbol{g}_{21}(\boldsymbol{r},\boldsymbol{r}',k)\,ds' + \frac{jk}{\eta} \int_{\sigma} \bar{\boldsymbol{G}}_{22}(\boldsymbol{r},\boldsymbol{r}',k)\cdot \boldsymbol{t}' E(s')\,ds' \tag{4b}$$

where $\boldsymbol{r}$ and $\boldsymbol{r}'=\boldsymbol{r}'(s')$ are the observation and the source points, respectively, $\boldsymbol{t}'=\boldsymbol{t}'(s')$ denotes the tangent vector at the source point, and $g_{11}, \boldsymbol{g}_{12}, \boldsymbol{g}_{21}, \bar{\boldsymbol{G}}_{22}$ are Green's functions for the resonator Ω. These functions may be represented as eigenfunction expansions, using the eigenfunctions and the eigenvalues of the problems:

$$\nabla^2\phi_m + h_m'^2\phi_m = 0 \qquad (\phi_m = 0 \text{ at } \partial\Omega) \tag{5a}$$

$$\nabla^2\psi_m + h_m^2\psi_m = 0 \qquad \left(\frac{\partial\psi_m}{\partial \boldsymbol{\nu}} = 0 \text{ at } \partial\Omega\right) \tag{5b}$$

$$\int_{\Omega} |\phi_m|^2\,d\Omega = 1 \qquad \int_{\Omega} |\psi_m|^2\,d\Omega = 1. \tag{5c}$$

The expressions for $g_{11}, \boldsymbol{g}_{12}, \boldsymbol{g}_{21}, \bar{\boldsymbol{G}}_{22}$ are

$$g_{11}(\boldsymbol{r},\boldsymbol{r}',k) = \sum_m \frac{\psi_m(\boldsymbol{r})\psi_m(\boldsymbol{r}')}{h_m^2 - k^2} - \frac{1}{k^2\Omega} \tag{6a}$$

$$\boldsymbol{g}_{12}(\boldsymbol{r},\boldsymbol{r}',k) = -\boldsymbol{z}\times\nabla' g_{11}(\boldsymbol{r},\boldsymbol{r}',k) \tag{6b}$$

$$\boldsymbol{g}_{21}(\boldsymbol{r},\boldsymbol{r}',k) = -\boldsymbol{g}_{12}(\boldsymbol{r}',\boldsymbol{r},k) \tag{6c}$$

$$\bar{\boldsymbol{G}}_{22}(\boldsymbol{r},\boldsymbol{r}',k) = -\frac{1}{k^2}\nabla\nabla' \sum_m \frac{\phi_m(\boldsymbol{r})\phi_m(\boldsymbol{r}')}{h_m'^2} + \sum_m \frac{\boldsymbol{e}_m(\boldsymbol{r})\boldsymbol{e}_m(\boldsymbol{r}')}{h_m^2 - k^2} \tag{6d}$$

where

$$\boldsymbol{e}_m = -\frac{\boldsymbol{z}\times\nabla\psi_m}{h_m}. \tag{7}$$

Formulas (4)–(7) may be deduced in many ways. The shortest one, probably, consists in determining them by duality from the general representation of fields in cylindrical regions, bounded by electric walls [15, sec. 13.2]. This derivation is straightforward, as it needs only to particularize the general formulas given in [15] to time-harmonic and z-independent sources. When Ω is circular or rectangular $\psi_m, \phi_m, h_m, h_m'$ are known, and their expressions can be found in many textbooks [e.g. 16]. It is worth noting that the last term in (6a) corresponds to the zero frequency eigenvalue occurring in the Neumann's problem (5b) ($h_0=0$, $\psi_0=\Omega^{-1/2}$).

As stated by the equivalence theorem, $\boldsymbol{E}$ and $\boldsymbol{H}$ differ from zero inside S and are zero outside. Therefore the fields at the boundary of the planar circuit must be deduced from (4a) and (4b) as limits for $\boldsymbol{r}$ tending to the boundary from the inside of S. For this reason the boundary condition on the magnetic field is

$$\boldsymbol{t}\cdot \lim_{\boldsymbol{r}\to\boldsymbol{r}_0} \boldsymbol{H}(\boldsymbol{r}) = -\sum_{i=1}^{N} \frac{I_i}{W_i} u_i(s) \qquad (\boldsymbol{r}\in S, \forall \boldsymbol{r}_0 \in \sigma). \tag{8}$$

It is stressed that the discontinuities in surface Green's integrals depend on the singularities of the Green's functions when $R=|\boldsymbol{r}-\boldsymbol{r}'|\to 0$. Therefore, if series (6) are truncated, one obtains poor approximations of $\boldsymbol{E}$ and $\boldsymbol{H}$ near σ, since the truncation destroys the singularities. On the other hand, (8) plays a fundamental role in setting up our algorithm, so that a good approximation of the field at σ is very important. For this reason it is mandatory to modify (6), extracting the singular terms from the Green's functions and expressing them is closed form. The extraction requires rewriting the fundamental functions g_{11} and $\bar{\boldsymbol{G}}_{22}$ as follows:

$$g_{11}(\boldsymbol{r},\boldsymbol{r}',k) = -\frac{1}{k^2\Omega} + g_{11}^0(\boldsymbol{r},\boldsymbol{r}') + k^2 \sum_m \frac{\psi_m(\boldsymbol{r})\psi_m(\boldsymbol{r}')}{h_m^2(h_m^2 - k^2)} \tag{9a}$$

$$\bar{\boldsymbol{G}}_{22}(\boldsymbol{r},\boldsymbol{r}',k) = -\frac{1}{k^2}\nabla\nabla' g_{22}^0(\boldsymbol{r},\boldsymbol{r}') + \bar{\boldsymbol{G}}_{22}^0(\boldsymbol{r},\boldsymbol{r}') + k^2 \sum_m \frac{\boldsymbol{e}_m(\boldsymbol{r})\boldsymbol{e}_m(\boldsymbol{r}')}{h_m^2(h_m^2 - k^2)} \tag{9b}$$

where

$$g_{11}^0 = \sum_m \frac{\psi_m(\boldsymbol{r})\psi_m(\boldsymbol{r}')}{h_m^2} \qquad g_{22}^0 = \sum_m \frac{\phi_m(\boldsymbol{r})\phi_m(\boldsymbol{r}')}{h_m'^2}$$

$$\bar{\boldsymbol{G}}_{22}^0 = \sum_m \frac{\boldsymbol{e}_m(\boldsymbol{r})\boldsymbol{e}_m(\boldsymbol{r}')}{h_m^2}. \tag{10}$$

TABLE I
g_{11}^0, g_{22}^0, AND $\bar{G}_{22}^0$ FOR A TWO-DIMENSIONAL RESONATOR OF CIRCULAR CROSS SECTION

$$g_{11}^{\circ}(r,\phi,r',\phi') = \frac{2(r^2+r'^2)-3a^2}{8\pi a^2} - \frac{1}{2\pi}\ln\frac{R(r'R_1/a)}{a^2}$$

$$g_{22}^{\circ}(r,\phi,r',\phi') = \frac{1}{2\pi}\ln\frac{r'R_1}{aR}$$

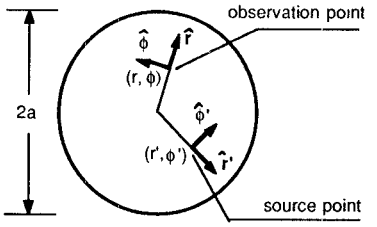

$$\bar{G}_{22}^{\circ}(r,\phi,r',\phi') = \frac{\hat{r}\hat{r}'}{8\pi}\left[2C\ln\frac{r'R_1}{aR} + \frac{(r^2+r'^2)C-2rr'}{R^2} + \frac{(r^2+r'^2+4a^2)C-2rr'}{(r'R_1/a)^2} - \frac{(a^2+r^2)(a^2+r'^2)}{r^2r'^2}\left(LC-AS+\frac{rr'}{(r'R_1/a)^2}\right)\right] +$$

$$+\frac{\hat{\phi}\hat{r}'}{8\pi}\left[-2S\ln\frac{r'R_1}{aR} + S\frac{r^2-r'^2}{R^2} + S\frac{r^2+r'^2-2a^2}{(r'R_1/a)^2} - \frac{(a^2-r^2)(a^2+r'^2)}{r^2r'^2}(LS+AC)\right] +$$

$$+\frac{\hat{r}\hat{\phi}'}{8\pi}\left[2S\ln\frac{r'R_1}{aR} + S\frac{r^2-r'^2}{R^2} - S\frac{r^2+r'^2-2a^2}{(r'R_1/a)^2} + \frac{(a^2+r^2)(a^2-r'^2)}{r^2r'^2}(LS+AC)\right] +$$

$$+\frac{\hat{\phi}\hat{\phi}'}{8\pi}\left[2C\ln\frac{r'R_1}{aR} - \frac{(r^2+r'^2)C-2rr'}{R^2} + \frac{(r^2+r'^2-2a^2)(rr'/a^2-C)}{(r'R_1/a)^2} - \frac{rr'}{a^2} - \frac{(a^2-r^2)(a^2-r'^2)}{r^2r'^2}\left(LC-AS+\frac{rr'}{a^2}\right)\right]$$

$$R = \sqrt{r^2+r'^2-2rr'C} \qquad R_1 = \sqrt{r^2+a^4/r'^2-2ra^2C/r'}$$

$$C = \cos(\phi-\phi') \qquad S = \sin(\phi-\phi') \qquad L = \ln\frac{r'R_1}{a^2} \qquad A = \mathrm{tg}^{-1}\frac{rr'S}{a^2-rr'C}$$

TABLE II
g_{11}^0, g_{22}^0, AND $\bar{G}_{22}^0$ FOR A TWO-DIMENSIONAL RESONATOR OF RECTANGULAR CROSS SECTION

$$g_{11}^{\circ}(x,y,x',y') = \frac{a}{3b} + \frac{x^2+x'^2}{2ab} - \frac{|X_0^0|+|X_0^1|}{2\pi} - \frac{1}{4\pi}\sum_{m=-\infty}^{+\infty}\sum_{p,q=0}^{1}\ln T_m^{pq}$$

$$g_{22}^{\circ}(x,y,x',y') = -\frac{1}{4\pi}\sum_{m=-\infty}^{+\infty}\sum_{p,q=0}^{1}(-1)^{p+q}\ln T_m^{pq}$$

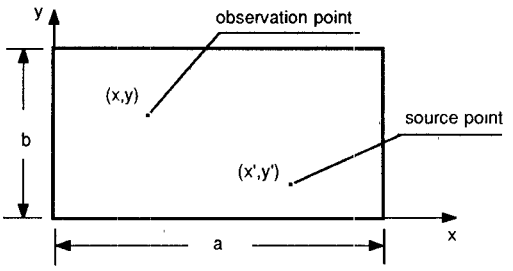

$$\bar{G}_{22}^{\circ}(x,y,x',y') = \frac{\hat{x}\hat{x}}{4\pi}\sum_{m=-\infty}^{+\infty}\sum_{p,q=0}^{1}(-1)^q\left[\frac{1}{2}\ln T_m^{pq} - |X_m^p|E_m^p\frac{\cos Y^q - E_m^p}{T_m^{pq}}\right] - \frac{\hat{x}\hat{y}}{4\pi}\sum_{m=-\infty}^{+\infty}\sum_{p,q=0}^{1}(-1)^p X_m^p E_m^p\frac{\sin Y^q}{T_m^{pq}} +$$

$$-\frac{\hat{y}\hat{x}}{4\pi}\sum_{m=-\infty}^{+\infty}\sum_{p,q=0}^{1}(-1)^q X_m^p E_m^p\frac{\sin Y^q}{T_m^{pq}} + \frac{\hat{y}\hat{y}}{4\pi}\left(\sum_{m=-\infty}^{+\infty}\sum_{p,q=0}^{1}(-1)^p\left[\frac{1}{2}\ln T_m^{pq} + |X_m^p|E_m^p\frac{\cos Y^q - E_m^p}{T_m^{pq}}\right] - \frac{4\pi xx'}{ab} + 2(|X_0^0| - |X_0^1|)\right)$$

$$X_m^p = \frac{\pi}{b}[x+(-1)^p x' - 2am] \qquad Y^q = \frac{\pi}{b}[y+(-1)^q y'] \qquad E_m^p = \exp(-|X_m^p|) \qquad T_m^{pq} = 1 - 2E_m^p\cos Y^q + (E_m^p)^2$$

Singularities are due to the term $\ln T_0^{11}$ which diverges like $\ln R$ $\qquad$ $\hat{x}$, $\hat{y}$ = unit vectors

It can be easily verified that g_{11} and g_{11}^0 are the Green's functions for the scalar wave equation and for the Poisson equation in two dimensions, respectively. As they exhibit the same singularity, it is evident that the only singular term on the r.h.s. in (9a) is g_{11}^0. Expression (9b) is discussed in [17], where it is shown that the singularities are contained in g_{22}^0 and $\bar{G}_{22}^0$. Functions g_{11}^0, g_{22}^0, and $\bar{G}_{22}^0$ diverge as $\ln R$.

The extraction of singularities requires the transformation of the series (10) so as to evidence the logarithmic terms. The transformation can be done when Ω is rectangular or circular, the cases we are interested in. As the procedure is very cumbersome, for the sake of brevity we limit ourselves to the results in Tables I and II. We note that: i) $g_{11}^0, g_{22}^0, \bar{G}_{22}^0$ are given in closed form (Ω circular) or in the form of very rapidly converging series (Ω rectangular); ii) as a consequence of the extraction of the singular terms, the series in (9a) and (9b) represent continuous functions and converge quite rapidly [17], [18], so that they can be truncated without worries; and iii) after truncation expressions (9a) and (9b) become rational functions of k. This last fact constitutes a further advantage of considering S as embedded in the outer resonator Ω. In fact, using Green's functions which are rational functions of k permits the algebraic manipulations, developed in the next section, that lead to the wide-band expression of the Z parameters.

In the following the number of terms retained in the summations in (9a) and (9b) will be denoted by M. As discussed in Section V, in our application the value of M is reasonably small since, in order to have a good accuracy, it is sufficient that h_M exceeds only slightly the value of k at the maximum frequency of interest.

After introducing (9) into (4) we obtain the two basic equations for this theory. One is obtained imposing condition (8), the other calculating $E(s)$ from (4a) as the limiting value of the electric field $E(\boldsymbol{r})$ when $\boldsymbol{r}$ tends to a point on ∂S from the inside of S. Particular care is required in the calculation of the limits of the integrals involving the singular parts of the Green's functions [19]. The calculation of the limits is reported in Appendix I.

The two basic equations are

$$\frac{\partial}{\partial s}\int_\sigma g_{22}^0(s,s')\frac{\partial}{\partial s'}E(s')\,ds' + k^2\int_\sigma \boldsymbol{t}\cdot\bar{G}_{22}^0(s,s')\cdot\boldsymbol{t}'E(s')\,ds' + k^2\sum_{m=1}^{M}\frac{a_m}{h_m^2}\boldsymbol{t}\cdot\boldsymbol{e}_m(s)$$
$$= j\eta k\sum_{\iota=1}^{N}\frac{I_\iota}{W_\iota}\left[\frac{u_\iota(s)}{2} - \int_{W_\iota}\boldsymbol{t}\cdot\boldsymbol{z}\times\nabla g_{11}^0(s',s)\,ds' + k^2\sum_{m=1}^{M}\frac{\boldsymbol{t}\cdot\boldsymbol{e}_m(s)}{h_m\left(h_m^2-k^2\right)}\int_{W_\iota}\psi_m(s')\,ds'\right] \quad (11)$$

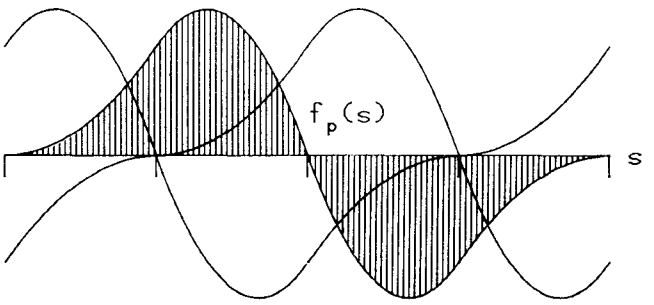

Fig. 2. A generic zero-mean base function.

for values of s corresponding to points of σ and

$$E(s) = j\eta k\sum_{\iota=1}^{N}\frac{I_\iota}{W_\iota}\left[\frac{W_\iota}{k^2\Omega} - \int_{W_\iota} g_{11}^0(s,s')\,ds' - k^2\sum_{m=1}^{M}\frac{\psi_m(s)}{h_m^2\left(h_m^2-k^2\right)}\int_{W_\iota}\psi_m(s')\,ds'\right] + \frac{E(s)}{2}u_\sigma(s) - \int_\sigma \boldsymbol{z}\times\nabla' g_{11}^0(s,s')\cdot\boldsymbol{t}'E(s')\,ds' + \sum_{m=1}^{M}\frac{a_m}{h_m}\psi_m(s) \quad (12)$$

for any value of s, where $u_\sigma(s)=1$ over σ, $u_\sigma(s)=0$ elsewhere, and

$$a_m = \frac{k^2}{h_m^2-k^2}\int_\sigma \boldsymbol{t}\cdot\boldsymbol{e}_m(s)E(s)\,ds. \quad (13)$$

In (11)–(13) the source and the observation points are indicated by their coordinates s, s' to put into evidence that both points are located on the boundary. The dash on the integral symbol denotes the "principal value."

III. Determination of the Z Matrix

For a given set of currents, (11) permits the determination of the unknown function $E(s)$ over σ. Introducing this function on the r.h.s. of (12), it is possible to find the electric field all over ∂S. Substituting this into

$$V_\iota = -\frac{d}{W_\iota}\int_{W_\iota} E(s)\,ds \quad (14)$$

the voltages $V_1, V_2, \cdots, V_N$ at the ports are obtained as function of the currents.

Assuming that, in general, σ consists of K separated parts $\sigma_1, \sigma_2, \cdots, \sigma_K$ (see Fig. 1(b)), the unknown function is expressed as

$$E(s) = \sum_{k=1}^{K} b_k' f_k'(s) + \sum_{p=1}^{P} b_p f_p(s) \qquad (\text{over } \sigma) \quad (15)$$

where f_k' and f_p are base functions and b_k', b_p are unknown coefficients. Functions f_k' are defined as follows:

$$f_k' = 1 \quad \text{for} \quad s\in\sigma_k; \qquad f_k' = 0 \quad \text{elsewhere.} \quad (16)$$

Any of the functions f_p has zero mean-value (see Fig. 2) and its support belongs to only one of the lines σ_k.

TABLE III
EXPRESSIONS OF THE ELEMENTS OF THE MATRICES USED IN (17) AND (22)

$$C_{pq} = \int_{\sigma}\int_{\sigma} \frac{\partial f_p(s)}{\partial s}\, g_{22}^{\circ}(s,s')\, \frac{\partial f_q(s')}{\partial s'}\, ds\, ds'$$

$$L'_{pq} = \int_{\sigma}\int_{\sigma} f_p(s)\, \mathbf{t}\cdot \bar{\mathbf{G}}_{22}^{\circ}(s,s')\cdot \mathbf{t}'\, f_q(s')\, ds\, ds'$$

$$Q'_{pi} = \frac{1}{W_i}\int_{\sigma}\left[\oint_{W_i} \mathbf{t}\cdot \mathbf{z}\times\nabla g_{11}^{\circ}(s',s)\, f_p(s)\, ds' - \frac{u_i(s)\, f_p(s)}{2}\right] ds =$$

$$= \frac{1}{W_i}\int_{W_i}\left[\oint_{\sigma} \mathbf{t}'\cdot \mathbf{z}\times\nabla' g_{11}^{\circ}(s,s')\, f_p(s')\, ds' - \frac{f_p(s)}{2}\right] ds$$

$$R'_{pm} = \frac{1}{h_m^2}\int_{\sigma} f_p(s)\, \mathbf{t}\cdot \mathbf{e}_m(s)\, ds$$

$$S_{hk} = \int_{\sigma_h}\int_{\sigma_k} \mathbf{t}\cdot \bar{\mathbf{G}}_{22}^{\circ}(s,s')\cdot \mathbf{t}'\, ds\, ds' = S_h\delta_{hk} - \frac{S_h S_k}{\Omega}$$

$$T_{ij} = \frac{1}{W_i W_j}\int_{W_i}\int_{W_j} g_{11}^{\circ}(s,s')\, ds\, ds'$$

$$F_{mi} = \frac{1}{h_m W_i}\int_{W_i} \psi_m(s)\, ds$$

$$L''_{kq} = \int_{\sigma_k}\int_{\sigma} \mathbf{t}\cdot \bar{\mathbf{G}}_{22}^{\circ}(s,s')\cdot \mathbf{t}'\, f_q(s')\, ds\, ds'$$

$$Q''_{ki} = \frac{1}{W_i}\int_{\sigma_k}\left[\oint_{W_i} \mathbf{t}\cdot \mathbf{z}\times\nabla g_{11}^{\circ}(s',s)\, ds' - \frac{u_i(s)}{2}\right] ds =$$

$$= \frac{1}{W_i}\int_{W_i,\sigma_k}\left[\oint \mathbf{t}'\cdot \mathbf{z}\times\nabla' g_{11}^{\circ}(s,s')\, ds' - \frac{f'_k(s)}{2}\right] ds = \frac{S_k}{\Omega}$$

$$R''_{km} = \frac{1}{h_m^2}\int_{\sigma_k} \mathbf{t}\cdot \mathbf{e}_m(s)\, ds$$

$$(\mathbf{S}^{-1})_{hk} = \frac{\delta_{hk}}{S_h} + \frac{1}{S}$$

$i,j = 1,2,\ldots,N$ $\quad h,k = 1,2,\ldots,K$ $\quad m,n = 1,2,\ldots,M$ $\quad p,q = 1,2,\ldots,P$ $\quad \delta_{hk}$ = Kronecker symbol

Introducing (15) into (11) and (13), and applying the Galerkin's procedure, the following system of matrix equations is obtained:

$$-k^2\boldsymbol{R}'\boldsymbol{a} + (\boldsymbol{C} - k^2\boldsymbol{L}')\boldsymbol{b} - k^2\boldsymbol{L}''_T\boldsymbol{b}' = j\eta k(\boldsymbol{Q}' - k^2\boldsymbol{R}'\Delta\boldsymbol{F})\boldsymbol{i} \tag{17a}$$

$$-k^2\boldsymbol{R}''\boldsymbol{a} - k^2\boldsymbol{L}''\boldsymbol{b} - k^2\boldsymbol{S}\boldsymbol{b}' = j\eta k(\boldsymbol{Q}'' - k^2\boldsymbol{R}''\Delta\boldsymbol{F})\boldsymbol{i} \tag{17b}$$

$$(\boldsymbol{U} - k^2\boldsymbol{D}')\boldsymbol{a} - k^2\boldsymbol{R}'_T\boldsymbol{b} - k^2\boldsymbol{R}''_T\boldsymbol{b}' = \boldsymbol{0} \tag{17c}$$

where $\boldsymbol{U}$ is the $M\times M$ unit matrix, $\boldsymbol{a} = (a_1, a_2, \cdots, a_M)$, $\boldsymbol{b} = (b_1, b_2, \cdots, b_P)$,

$$\boldsymbol{b}' = (b'_1, b'_2, \cdots, b'_K), \qquad \boldsymbol{i} = (I_1, I_2, \cdots, I_N),$$

$$\boldsymbol{D}' = \operatorname{diag}\left[h_1^{-2}, h_2^{-2}, \cdots, h_M^{-2}\right]$$

$$\Delta = \operatorname{diag}\left[h_1^2/(h_1^2 - k^2), \cdots, h_M^2/(h_M^2 - k^2)\right] \tag{18}$$

and the elements of the other matrices are defined in Table III. The subscript T denotes the transpose. Note that all the matrices listed in Table III are k-independent and that the elements of $\boldsymbol{S}$ and $\boldsymbol{Q}''$ are related to the areas $S, S_1, S_2, \cdots, S_K$, defined in Fig. 1(b) (see Appendix II).

From (17b) we obtain

$$\boldsymbol{b}' = -\boldsymbol{S}^{-1}[\boldsymbol{R}''\boldsymbol{a} + \boldsymbol{L}''\boldsymbol{b}] - \frac{j\eta}{k}\boldsymbol{S}^{-1}\boldsymbol{Q}''\boldsymbol{i} + j\eta k\boldsymbol{S}^{-1}\boldsymbol{R}''\Delta\boldsymbol{F}\boldsymbol{i}. \tag{19}$$

Explicit expressions of the elements of $\boldsymbol{S}^{-1}$ are easily found (see Table III and Appendix II).

On substitution of (19) into (17a) and (17c) the following matrix equation is obtained:

$$\left(\begin{bmatrix} \boldsymbol{U} & \boldsymbol{0} \\ \boldsymbol{0} & \boldsymbol{C} \end{bmatrix} - k^2\begin{bmatrix} \boldsymbol{D} & \boldsymbol{R}_T \\ \boldsymbol{R} & \boldsymbol{L} \end{bmatrix}\right)\begin{bmatrix} \boldsymbol{a} \\ \boldsymbol{b} \end{bmatrix} = j\eta k\left(\begin{bmatrix} \boldsymbol{H} \\ \boldsymbol{Q} \end{bmatrix} - k^2\begin{bmatrix} \boldsymbol{D} - \boldsymbol{D}' \\ \boldsymbol{R} \end{bmatrix}\Delta\boldsymbol{F}\right)\boldsymbol{i} \tag{20}$$

where

$$\boldsymbol{D} = \boldsymbol{D}' - \boldsymbol{R}''_T\boldsymbol{S}^{-1}\boldsymbol{R}'' \tag{21a}$$

$$\boldsymbol{R} = \boldsymbol{R}' - \boldsymbol{L}''_T\boldsymbol{S}^{-1}\boldsymbol{R}'' \tag{21b}$$

$$\boldsymbol{L} = \boldsymbol{L}' - \boldsymbol{L}''_T\boldsymbol{S}^{-1}\boldsymbol{L}'' \tag{21c}$$

$$\boldsymbol{H} = -\boldsymbol{R}''_T\boldsymbol{S}^{-1}\boldsymbol{Q}'' \tag{21d}$$

$$\boldsymbol{Q} = \boldsymbol{Q}' - \boldsymbol{L}''_T\boldsymbol{S}^{-1}\boldsymbol{Q}''. \tag{21e}$$

Before discussing the solution of (20), we observe that substituting (12) into (14) and using (15) and (19), the

voltage vector $v=(V_1,V_2,\cdots,V_N)$ can be represented as

$$v=\frac{\eta d}{jk}\left[\frac{1}{\Omega}I+Q_T''S^{-1}Q''\right]i + j\eta kd\left[T+\left(k^2F_TD'-H_T\right)\Delta F\right]i + d\begin{bmatrix}H-F\\ \cdots\\ Q\end{bmatrix}_T\begin{bmatrix}a\\ \cdots\\ b\end{bmatrix} \quad (22)$$

where I is an $N\times N$ matrix having unit elements, and T is defined in Table III.

To solve (20) we observe that (see appendix IV)

$$\left(\begin{bmatrix}U & 0\\ \cdots & \cdots\\ 0 & C\end{bmatrix}-k^2\begin{bmatrix}D & R_T\\ \cdots & \cdots\\ R & L\end{bmatrix}\right)^{-1} = \begin{bmatrix}A\\ \cdots\\ B\end{bmatrix}\operatorname{diag}\left(\frac{1}{\kappa_r^2-k^2}\right)\begin{bmatrix}A\\ \cdots\\ B\end{bmatrix}_T \quad (23)$$

where the quantities κ_r are the eigenvalues of the problem

$$\left(\begin{bmatrix}U & 0\\ \cdots & \cdots\\ 0 & C\end{bmatrix}-\kappa_r^2\begin{bmatrix}D & R_T\\ \cdots & \cdots\\ R & L\end{bmatrix}\right)\begin{bmatrix}a\\ \cdots\\ b\end{bmatrix}_r=0 \qquad (r=1,2,\cdots,P+M) \quad (24)$$

and (A,B) denotes the matrix whose columns are the eigenvectors $(a,b)_r$ normalized according to (A3). Since the matrices

$$\begin{bmatrix}U & 0\\ \cdots & \cdots\\ 0 & C\end{bmatrix} \qquad \begin{bmatrix}D & R_T\\ \cdots & \cdots\\ R & L\end{bmatrix} \quad (25)$$

are positive definite (see Appendix III), the eigenvectors are real and the eigenvalues are real positive. Using (23) we obtain, from (20),

$$\begin{bmatrix}a\\ \cdots\\ b\end{bmatrix}=\begin{bmatrix}A\\ \cdots\\ B\end{bmatrix}\operatorname{diag}\left(\frac{1}{\kappa_r^2-k^2}\right)\begin{bmatrix}A\\ \cdots\\ B\end{bmatrix}_T \cdot j\eta k\left(\begin{bmatrix}H\\ \cdots\\ Q\end{bmatrix}-k^2\begin{bmatrix}D-D'\\ \cdots\\ R\end{bmatrix}\Delta F\right)i. \quad (26)$$

On substitution into (22) and after some manipulation involving formulas (A1) and (A5)–(A9), we obtain the voltage/current relationship in the form $v=Zi$, where the Z matrix is given by the expression

$$Z=\frac{1}{jk}\frac{\eta d}{S}I+jk\eta d\Lambda+jk^3\frac{\eta}{d}V\operatorname{diag}\left(\frac{1}{\kappa_r^2\left(\kappa_r^2-k^2\right)}\right)V_T \quad (27)$$

where

$$\Lambda=T+Q_TC^{-1}Q+H_TH-F_TH-H_TF \quad (28)$$

$$V=d\left(H_T-F_T\right)A+dQ_TB. \quad (29)$$

IV. Discussion

The eigenvalue problem (24) is equivalent to the solution of (20) in the case $i=0$. Equation (15), together with (19) with $i=0$, yields a field distribution $E^{(r)}(s)$ for each eigenvector $(a,b)_r$. These fields represent the eigensolutions of the homogeneous equation obtained from (11) when the exciting currents are zero. The eigensolutions occur at some particular values of k, corresponding to the eigenvalues κ_r.

It is realized that solving the homogeneous equation means finding the resonances of the planar circuit when the ports are terminated by magnetic walls. On the other hand it is pointed out that the solution of the homogeneous equation also yields the resonances occurring in the outer regions $S_1,S_2,\cdots,S_K$. In fact it could be verified that, if the determination of the field in these regions were of interest, the above theory should be applied, with the only difference of a sign reversal in t and a different procedure of limit in the representation the boundary condition (8) (r should tend to σ from *the outside of* S rather than from the inside). When the currents are zero, an integrodifferential equation identical to (11) should be obtained. For this reason eigenvalues κ_r and eigenvectors $(a,b)_r$ correspond to resonances occurring either inside or outside the region S.

The voltages at the rth resonance are obtained from (22), putting $i=0$ and introducing the rth eigenvector. This yields

$$v_r=d\left(H_T-F_T\right)a_r+dQ_Tb_r. \quad (30)$$

These vectors are the columns of the matrix V (see. (29)), so that the generic element V_{ir} represents the voltage at the ith port, for the rth resonance. Apart from the approximations involved in the numerical algorithm, the voltage vectors corresponding to spurious resonances are zero as the electric field for such resonances is zero inside S. Therefore the spurious resonances have no influence in the calculation of the Z parameters, so that the voltage vectors and the elements in the diagonal matrix corresponding to them can be completely disregarded in (27). Actually, for spurious resonances the numerical algorithm yields nonzero vectors which, however, are easily detected since they are characterized by very small elements. After the identification and elimination of the spurious resonances, the dimensions of the matrix V are reduced from $N\times(P+M)$ to $N\times Q$, by retaining the Q significant columns only. At the same time the number of elements in the diagonal matrix is reduced to Q by retaining the terms containing the Q significant eigenvalues only. These eigenvalues represent the resonating wavenumbers of the open-circuited planar circuit, i.e., the quantities denoted by k_q in the Introduction. The elements of the matrix Z given by (27) have the form (1) and the coefficients involved in the summation have the meaning given in the Introduction.

V. Numerical Implementation and Examples

The algorithm described in the preceding sections was implemented in a user-oriented computer program, named ANAPLAN, whose distinguishing feature is the short com-

puter time. In the following an outline of the program is given. Details of the program can be found in [20].

As a first step in the computing procedure, the boundary ∂S of the planar circuit is generated interactively through a graphic module, starting from a rectangular or a circular shape. The modifications of the starting contour are represented by polygonals, which constitute the discretization of the lines σ_k.

In the implementation of the algorithm we use base functions consisting of interlaced, piecewise-parabolic functions, each supported by four adjacent segments of σ_k and going to zero, together with their derivative, at the extremes of its support (see Fig. 2). Different functions, supported by three segments only, are used in proximity to the extremes of those lines σ_k that depart from $\partial\Omega$. These functions are piecewise parabolic too, but they differ from zero at the extreme coincident with $\partial\Omega$. These functions make it possible to represent $E(s)$ at the extremes of each line σ_k, where it might differ from zero. Since parabolic base functions are used, a small number of them is sufficient for an accurate representation of the field. Actually, it was observed that very good results are obtained, provided the length of no segment of the polygonals exceeds a quarter wavelength at the maximum frequency of interest. This condition is automatically verified since ANAPLAN checks the segmentation and subdivides any segments that are too long. A more dense segmentation is provided close to the possible edges of the lines σ_k, to allow for the rapid variation of the field which can occur there.

ANAPLAN automatically finds the number M of terms retained in the modal series (9) following the rule of thumb that the highest eigenvalue h_M must be about two times larger than the maximum value of k in the band of interest. We observed experimentally that this rule ensures a good accuracy in the evaluation of the Green's functions throughout the whole frequency band.

The next step is the calculation of all the coefficients of the matrices defined in Table III. The contributions to the integrals arising from the singular terms contained in g_{11}^0, g_{22}^0, $\bar{G}_{22}$ are calculated analytically. Contributions to the integrals coming from the regular parts of the Green's functions, as well as the other integrals, are evaluated numerically.

Once matrices (25) have been calculated, the eigenvectors and eigenvalues of (24) are determined, using standard library routines. Finally matrices (28) and (29) are evaluated and the Z parameters (or the S parameters derived from them) are calculated using (1).

We report the results of the wide-band analysis of the planar circuit of Fig. 3. This circuit is a 3-dB hybrid coupler and has the same dimensions as the one snalyzed by Okoshi [5, pp. 113–117] using the contour integral method. Our analysis was performed in the $0 \sim 10$ GHz band. In this example, the starting contour is the external circle and the line σ is the inner contour. $P = 20$ base functions were used to represent the field at the inner contour. The value $M = 11$ was chosen by ANAPLAN. The obtained results are reported in Fig. 4, which shows

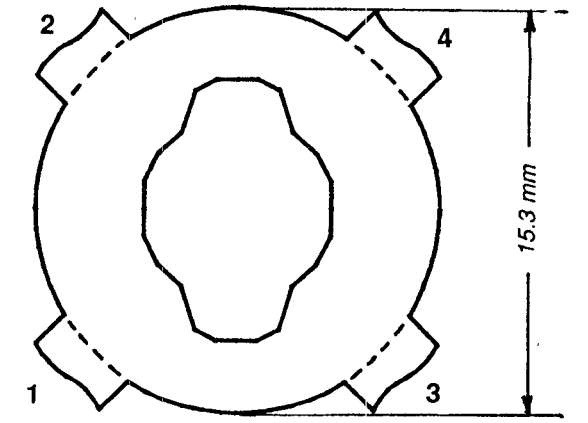

Fig. 3. The 3-dB hybrid coupler used in the test example. A more accurate definition of dimensions is given in [5, fig. 7.7]. Relative permittivity is $\epsilon_r = 2.35$.

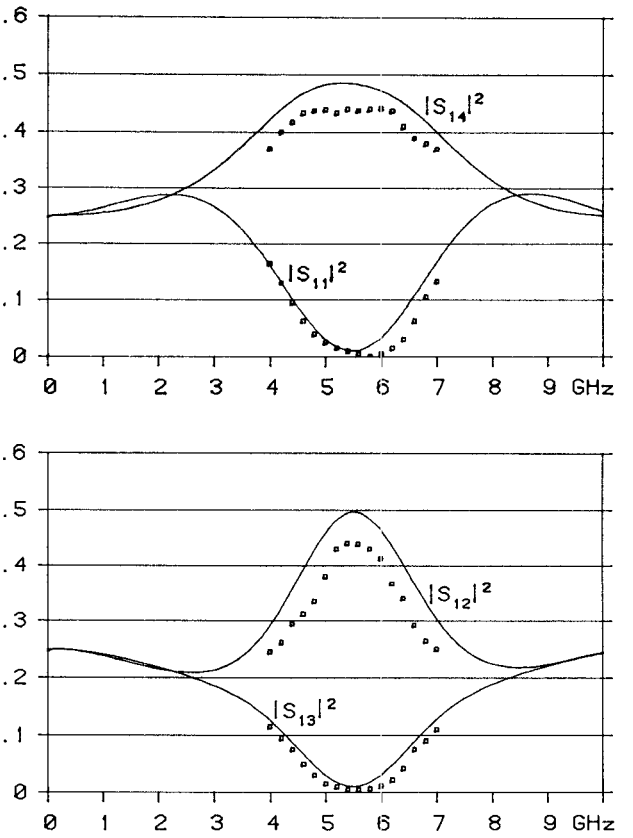

Fig. 4. Magnitudes of the S parameters of the circuit of Fig. 3 calculated by ANAPLAN. Squares represent experimental data reported in [5].

the squared magnitudes of the four scattering parameters (continous lines). The CPU time was about 5 s on a Digital VAX 8500 computer. About 3.5 s was required for the calculation of all the matrix elements listed in Table III, and a remaining 1.5 s was required for the solution of the eigenvalue problem and the calculation of the elements of the matrices Λ and V. The results of our analysis are practically coincident with the ones reported by Okoshi (differences on the plots are inappreciable). On the same figures are represented the experimental data reported by Okoshi [5, fig. 7.10(a)]. Differences are due to the fact that

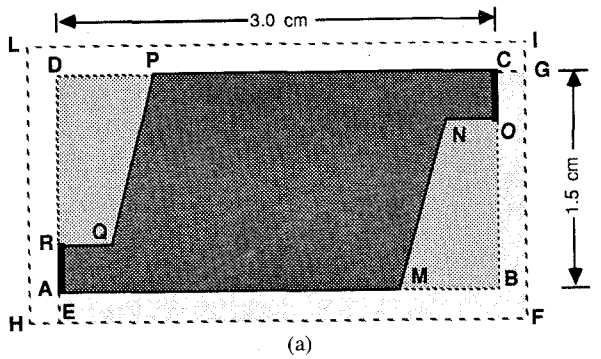

(a)

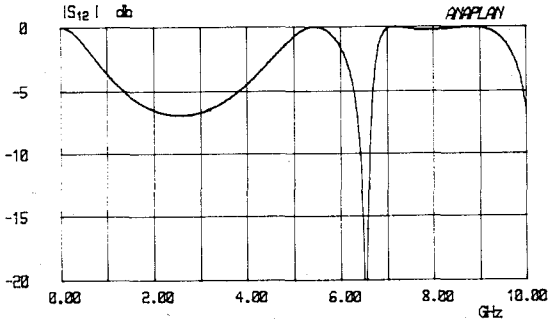

(b)

Fig. 5. (a) The geometry of the planar circuit enclosed in three different rectangular resonators. Relative permittivity is $\epsilon_r = 2.35$. (b) Magnitude of S_{12} computed by ANAPLAN.

losses are ignored in the analyses. It is pointed out that the quoted CPU time concerns the analysis in the *whole* 0 ~ 10 GHz band. For the same circuit, Okoshi reports a computer time of 4 s *per frequency* on a HITAC 8800 computer, and 50 frequency points at least should be considered for analyzing the circuit in the same band. Though these CPU times cannot be compared exactly, as they refer to different machines, they make it possible to appreciate the speed of our algorithm, since the computing powers of the two machines are comparable. It is observed that the computing time required by our algorithm is scarcely affected by the irregularities in the frequency response of the circuitto be analyzed, whereas in cases of irregular frequency responses the number of points to be considered in a frequency-by-frequency analysis should increase dramatically.

A further example concerns the circuit in Fig. 5(a), which was analyzed in the band 0 ~ 10 GHz, considering it as embedded in three different rectangles (ABCD, EFGD, HFIL). This example makes it possible to realize the advantage of having a part of the boundary coinciding with the external boundary $\partial\Omega$. The noncoincident part of the boundary (σ) consists of the lines MNO + PQR in the first case, of AMNOC + PQR in the second case, and of the whole boundary in the third case. In the three cases we had: $P = 12$, $M = 27$; $P = 20$, $M = 33$; and $P = 28$, $M = 37$. The increase in M derives from the increase in the size of Ω, which causes an increasing number of resonances of Ω to occur inside the band of interest. The results of the analyses, represented in Fig. 5(b), are indistinguishable in the three cases; this emphasizes that the accuracy of our method is unaffected by the choice of the outer contour $\partial\Omega$. This choice, on the contrary, has a large impact on the computing time, which in the three cases was 2.3 s, 6.3 s, and 12.2 s, respectively. Such results show the important time saving which is obtained in the analysis of shapes slightly differing from Ω. On the other hand, the maximum time of 12.2 s suggests the rapidity of the algorithm in cases where the circuit and the external resonator have no common boundary.

Appendix I
Calculation of Some Limits of Integrals Involving Singular Functions Occurring in the Derivation of (11) and (12)

All the following limits are calculated letting the observation point $\boldsymbol{r}$ tend to a point $\boldsymbol{r}_0$ of ∂S (or σ) from the inside of the region S.

The first limit is

$$L_1 = \boldsymbol{t}\cdot \lim_{r\to r_0}\int_\sigma \nabla\nabla' g_{22}^0(\boldsymbol{r},\boldsymbol{r}')\cdot \boldsymbol{t}' E(s')\,ds'$$

$$= \boldsymbol{t}\cdot \lim_{r\to r_0}\int_\sigma \nabla \frac{\partial}{\partial s'} g_{22}^0(\boldsymbol{r},\boldsymbol{r}') E(s')\,ds'$$

$$= -\boldsymbol{t}\cdot \lim_{r\to r_0}\int_\sigma \nabla g_{22}^0(\boldsymbol{r},\boldsymbol{r}')\frac{\partial}{\partial s'} E(s')\,ds'$$

$$(\boldsymbol{r}_0 = \boldsymbol{r}_0(s) \in \sigma)$$

where the transformation was performed integrating by parts and observing that σ (or its component parts) is either a closed line or a line with extremes on $\partial\Omega$, where g_{22}^0 is zero. As we have $g_{22}^0 = -\ln R/2\pi +$ regular function (see Tables I, II), we obtain

$$\nabla g_{22}^0(\boldsymbol{r},\boldsymbol{r}') = -\frac{\boldsymbol{r}-\boldsymbol{r}'}{2\pi R^2} + \text{regular function}.$$

Then, denoting by Δ an infinitesimal element of σ centered at $\boldsymbol{r}_0 = \boldsymbol{r}_0(s)$, we have

$$L_1 = \frac{\partial E(s)}{\partial s}\boldsymbol{t}\cdot \lim_{r\to r_0}\int_\Delta \frac{\boldsymbol{r}-\boldsymbol{r}'}{2\pi R^2}\,ds'$$

$$-\boldsymbol{t}\cdot \oint_\sigma \nabla g_{22}^0(\boldsymbol{r}_0,\boldsymbol{r}')\frac{\partial E(s')}{\partial s'}\,ds'$$

where

$$\oint_\sigma = \int_{\sigma-\Delta}.$$

Calculating the integral over Δ it is discovered that it is normal to $\boldsymbol{t}$. Therefore this integral does not contribute to L_1. Extracting ∇ from the last integral and observing that the logarithmic singularity of g_{22}^0 is integrable, we obtain

the result

$$L_1 = -\frac{\partial}{\partial s}\int_\sigma g_{22}^0(r_0, r')\frac{\partial E(s')}{\partial s'}\,ds'.$$

The second limit is

$$L_2 = t\cdot \lim_{r\to r_0}\int_{W_t} z\times\nabla g_{11}^0(r', r)\,ds' \qquad (r_0 = r_0(s)\in\sigma).$$

As we have $g_{11}^0 = -\ln R/2\pi$ + regular function (see Tables I, II), we obtain

$$\nabla g_{11}^0(r', r) = \frac{r-r'}{2\pi R^2} + \text{regular function}.$$

When $r_0 \in W_t$, we have

$$L_2 = t\cdot \lim_{r\to r_0}\int_\Delta z\times\frac{r-r'}{2\pi R^2}\,ds' + \oint_{W_t} t\cdot z\times\nabla g_{11}^0(r', r_0)\,ds'$$

$$= \frac{1}{2} + \oint_{W_t} t\cdot z\times\nabla g_{11}^0(r', r_0)\,ds'.$$

When $r_0 \notin W_t$ the term $1/2$ is missing and the integral is of the usual type.

The third limit is

$$L_3 = \lim_{r\to r_0}\int_\sigma t'\cdot z\times\nabla' g_{11}^0(r, r')E(s')\,ds' \qquad (r_0 = r_0(s)\in\partial S).$$

The calculation is similar to the previous one. When $r_0 \in \sigma$ we obtain

$$L_3 = -\frac{E(s)}{2} + \oint_\sigma t'\cdot z\times\nabla' g_{11}^0(r_0, r')E(s')\,ds'.$$

When $r_0 \notin \sigma$ the term $-E/2$ is missing and the integral is of the usual type.

The last limit is

$$L_4 = t\cdot \lim_{r\to r_0}\int_\sigma \bar{G}_{22}^0(r, r')\cdot t'E(s')\,ds'$$

$$= \int_\sigma t\cdot\bar{G}_{22}^0(r_0, r')\cdot t'E(s')\,ds'$$

since the integral is continuous across σ, due to the weakness of the logarithmic singularity of $\bar{G}_{22}^0$.

Appendix II

A. Expression for S_{hk} and $(S^{-1})_{hk}$

Using the modal representation of $\bar{G}_{22}^0$ we have

$$S_{hk} = \int_{\sigma_h}\int_{\sigma_k} t\cdot\sum_m \frac{e_m(s)e_m(s')}{h_m^2}\cdot t'\,ds\,ds'$$

$$= \oint_{\partial s_h}\oint_{\partial s_k} t\cdot\sum_m \frac{e_m(s)e_m(s')}{h_m^2}\cdot t'\,ds\,ds'$$

where the integrals are extended to the whole contours ∂S_h, ∂S_k, since $t\cdot e_m = 0$ on $\partial\Omega$. Using Stokes theorem and observing that $\nabla\times e_m = z h_m\psi_m$ we obtain

$$S_{hk} = \int_{S_h}\int_{S_k}\sum_m \psi_m(r)\psi_m(r')\,dS_h\,dS_k = \delta_{hk}S_h - \frac{S_hS_k}{\Omega}$$

due to the completeness relation:

$$\delta(r-r') = \frac{1}{\Omega} + \sum_m \psi_m(r)\psi_m(r').$$

The validity of the expression of $(S^{-1})_{hk}$ given in Table III is verified directly using $SS^{-1} = U$ and the geometrical relation $S = \Omega - S_1 - S_2 - \cdots - S_K$.

B. Expression for Q''_{kl}

Using the modal expansion of g_{11}^0 (see (10)) the second integral expression of Q''_{kl} given in Table III can be rewritten as

$$Q''_{kl} = \frac{1}{W_l}\int_{W_l}\left[\lim_{r\to r_0}\int_{\sigma_k} t'\cdot z\times\nabla'\sum_m \frac{\psi_m(r)\psi_m(r')}{h_m^2}\,ds'\right]ds \qquad (r_0\in W_l, r'\in\sigma_k).$$

Due to the boundary condition satisfied by ψ_m the integral over σ_k is transformed into a line integral over ∂S_k. Then, using Stokes theorem and observing that

$$z\cdot\nabla'\times\nabla'\times z\psi_m = -\nabla'^2\psi_m = h_m^2\psi_m$$

we obtain

$$Q''_{kl} = -\frac{1}{W_l}\int_{W_l}\left[\lim_{r\to r_0}\int_{S_k}\sum_m \psi_m(r)\psi_m(r')\,dS'_k\right]ds$$

$$= -\frac{1}{W_l}\int_{W_l}\left[\lim_{r\to r_0}\int_{S_k}\left(\delta(r-r') - \frac{1}{\Omega}\right)dS'_k\right]ds = \frac{S_k}{\Omega}$$

as r is external to S_k.

Moreover, starting from the expression of $(S^{-1})_{hk}$ given in Table III, it is easily verified that the following relation holds:

$$\left(Q''_T S^{-1} Q''\right)_{IJ} = \frac{1}{S} - \frac{1}{\Omega}. \tag{A1}$$

Appendix III

Positive Definiteness of Matrices (25)

The quadratic form associated to the first matrix is

$$f_1 = \sum_{m=1}^{M} a_m^2 + \sum_{p,q=1}^{P} b_p C_{pq} b_q.$$

Introducing the expression of C_{pq} given in Table III and using the modal expansion of g_{22}^0 (see (10)), after simple manipulations we obtain

$$f_1 = \sum_{m=1}^{M} a_m^2 + \sum_m\left[\sum_{p=1}^{P}\int_\sigma \frac{\partial f_p}{\partial s}\frac{\phi_m}{h'_m}\,ds\right]^2$$

which is always positive.

The quadratic form associated to the second matrix is

$$f_2 = \boldsymbol{a}_T\boldsymbol{D}\boldsymbol{a} + \boldsymbol{a}_T\boldsymbol{R}_T\boldsymbol{b} + \boldsymbol{b}_T\boldsymbol{R}\boldsymbol{a} + \boldsymbol{b}_T\boldsymbol{L}\boldsymbol{b}.$$

Introducing (21a)–(21c) we obtain

$$f_2 = \boldsymbol{a}_T\boldsymbol{D}'\boldsymbol{a} + \boldsymbol{a}_T\boldsymbol{R}'_T\boldsymbol{b} + \boldsymbol{a}_T\boldsymbol{R}''_T\boldsymbol{b}' + \boldsymbol{b}_T\boldsymbol{R}'\boldsymbol{a} + \boldsymbol{b}_T\boldsymbol{L}'\boldsymbol{b} + \boldsymbol{b}_T\boldsymbol{L}''_T\boldsymbol{b}' + \boldsymbol{b}'_T\boldsymbol{R}''\boldsymbol{a} + \boldsymbol{b}'_T\boldsymbol{L}''\boldsymbol{b} + \boldsymbol{b}'_T\boldsymbol{S}\boldsymbol{b}'$$

where

$$\boldsymbol{b}' = -\boldsymbol{S}^{-1}(\boldsymbol{R}''\boldsymbol{a} + \boldsymbol{L}''\boldsymbol{b}).$$

From the definition of the elements of the matrices $\boldsymbol{L}', \boldsymbol{L}'', \boldsymbol{S}, \boldsymbol{R}', \boldsymbol{R}''$, and considering the modal expansion of $\bar{\boldsymbol{G}}_{22}^0$ (see (10)) it is shown that

$$L'_{pq} = \sum_m h_m^2 R'_{mp} R'_{mq} \qquad L''_{kq} = \sum_m h_m^2 R''_{mk} R'_{mq}$$

$$S_{hk} = \sum_m h_m^2 R''_{mh} R''_{mk}.$$

On substitution into the last expression of f_2 after some manipulations we obtain

$$f_2 = \sum_{m=1}^{M} \left[\frac{a_m}{h_m} + h_m \sum_{p=1}^{P} \left(R'_{pm} b_p + R''_{pm} b'_p \right) \right]^2 + \sum_{m=M+1}^{\infty} h_m^2 \left(R'_{pm} b_p + R''_{pm} b'_p \right)^2$$

which is always positive.

APPENDIX IV

Some Useful Relations

Due to their positive definiteness (see Appendix III), matrices (25) can be simulataneously diagonalized using the matrix $(\boldsymbol{A}, \boldsymbol{B})$ having as columns the eigenvectors of the problem (24) [21, p. 106]. We have

$$\begin{bmatrix} \boldsymbol{A} \\ \cdots \\ \boldsymbol{B} \end{bmatrix}_T \begin{bmatrix} \boldsymbol{U} & \vdots & \boldsymbol{0} \\ \cdots & \vdots & \cdots \\ \boldsymbol{0} & \vdots & \boldsymbol{C} \end{bmatrix} \begin{bmatrix} \boldsymbol{A} \\ \cdots \\ \boldsymbol{B} \end{bmatrix} = \operatorname{diag}\left(\kappa_1^2, \kappa_2^2, \cdots, \kappa_{P+M}^2 \right) \quad \text{(A2)}$$

$$\begin{bmatrix} \boldsymbol{A} \\ \cdots \\ \boldsymbol{B} \end{bmatrix} \begin{bmatrix} \boldsymbol{D} & \vdots & \boldsymbol{R}_T \\ \cdots & \vdots & \cdots \\ \boldsymbol{R} & \vdots & \boldsymbol{L} \end{bmatrix} \begin{bmatrix} \boldsymbol{A} \\ \cdots \\ \boldsymbol{B} \end{bmatrix} = \boldsymbol{U}. \quad \text{(A3)}$$

Equation (A3) specifies the normalization of the eigenvectors. Using these expressions, (23) is verified easily.

Expression (A2) may be rewritten as

$$\boldsymbol{A}_T\boldsymbol{A} + \boldsymbol{B}_T\boldsymbol{C}\boldsymbol{B} = \operatorname{diag}\left\{ \kappa_1^2, \kappa_2^2, \cdots, \kappa_{M+P}^2 \right\} \quad \text{(A4)}$$

From the same expression it is obtained:

$$\begin{bmatrix} \boldsymbol{U} & \vdots & \boldsymbol{0} \\ \cdots & \vdots & \cdots \\ \boldsymbol{0} & \vdots & \boldsymbol{C} \end{bmatrix}^{-1} = \begin{bmatrix} \boldsymbol{A} \\ \cdots \\ \boldsymbol{B} \end{bmatrix} \operatorname{diag}\left\{ \kappa_1^{-2}, \kappa_2^{-2}, \cdots, \kappa_{M+P}^{-2} \right\} \begin{bmatrix} \boldsymbol{A} \\ \cdots \\ \boldsymbol{B} \end{bmatrix}_T$$

or

$$\begin{bmatrix} \boldsymbol{U} & \vdots & \boldsymbol{0} \\ \cdots & \vdots & \cdots \\ \boldsymbol{0} & \vdots & \boldsymbol{C} \end{bmatrix} \begin{bmatrix} \boldsymbol{A} \\ \cdots \\ \boldsymbol{B} \end{bmatrix} \operatorname{diag}\left\{ \kappa_1^{-2}, \kappa_2^{-2}, \cdots, \kappa_{M+P}^{-2} \right\} \begin{bmatrix} \boldsymbol{A} \\ \cdots \\ \boldsymbol{B} \end{bmatrix}_T = \begin{bmatrix} \boldsymbol{U} & \vdots & \boldsymbol{0} \\ \cdots & \vdots & \cdots \\ \boldsymbol{0} & \vdots & \boldsymbol{U} \end{bmatrix}.$$

This last expression yields the following useful relations:

$$\boldsymbol{A} \operatorname{diag}\left\{ \kappa_1^{-2}, \kappa_2^{-2}, \cdots, \kappa_{M+P}^{-2} \right\} \boldsymbol{A}_T = \boldsymbol{U} \quad \text{(A5)}$$

$$\boldsymbol{B} \operatorname{diag}\left\{ \kappa_1^{-2}, \kappa_2^{-2}, \cdots, \kappa_{M+P}^{-2} \right\} \boldsymbol{A}_T = \boldsymbol{0}. \quad \text{(A6)}$$

Analogously, starting from (A3) we obtain

$$(\boldsymbol{D}\boldsymbol{A} + \boldsymbol{R}_T\boldsymbol{B})\boldsymbol{A}_T = \boldsymbol{U} \qquad (\boldsymbol{D}\boldsymbol{A} + \boldsymbol{R}_T\boldsymbol{B})\boldsymbol{B}_T = \boldsymbol{0}.$$

Postmultiplying the latter of these equations by $\boldsymbol{C}\boldsymbol{B}$, using the expression of $\boldsymbol{B}_T\boldsymbol{C}\boldsymbol{B}$ deduced from (A4), and introducing the former, we obtain

$$(\boldsymbol{D}\boldsymbol{A} + \boldsymbol{R}_T\boldsymbol{B}) \operatorname{diag}\left(\kappa_1^2, \kappa_2^2, \cdots, \kappa_{M+P}^2 \right) = \boldsymbol{A}. \quad \text{(A7)}$$

Furthermore, in the derivation of (27), the following identities are used:

$$\operatorname{diag}\left(\frac{h_m^2}{h_m^2 - k^2} \right) = \boldsymbol{U} + k^2 \operatorname{diag}\left(\frac{1}{h_m^2 - k^2} \right) \quad \text{(A8)}$$

$$\operatorname{diag}\left(\frac{1}{\kappa_r^2 - k^2} \right) = \operatorname{diag}\left(\frac{1}{\kappa_r^2} \right) + k^2 \operatorname{diag}\left(\frac{1}{\kappa_r^2 \left(\kappa_r^2 - k^2 \right)} \right). \quad \text{(A9)}$$

REFERENCES

[1] G. Biorci and S. Ridella, "On the theory of distributed three-layer *N*-port networks," *Alta Frequenza*, vol. XXXVIII, pp. 615–622, Aug. 1969.

[2] B. Bianco and P. P. Civalleri, "Basic theory of three-layer *N*-port," *Alta Frequenza*, vol. XXXVIII, pp. 623–631, Aug. 1969.

[3] P. P. Civalleri and S. Ridella, "Impedance and admittance matrices of distributed three-layer *N*-port," *IEEE Trans. Circuit Theory*, vol. CT-17, pp. 392–398, Aug. 1970.

[4] T. Okoshi and T. Miyoshi, "The planar circuit—An approach to microwave integrated circuitry," *IEEE Trans. Microwave Theory Tech.*, vol. MTT-20, pp. 245–252, Apr. 1972.

[5] T. Okoshi, *Planar Circuits for Microwave and Lightwaves*. Berlin: Springer-Verlag, 1985.

[6] R. Sorrentino, "Planar circuits, waveguide models, and segmentation method," *IEEE Trans. Microwave Theory Tech.*, vol. MTT-33, pp. 1057–1066, Oct. 1985.

[7] I. Wolff and N. Knoppik, "Rectangular and circular disc capacitors and resonators," *IEEE Trans. Microwave Theory Tech.*, vol. MTT-22, pp. 857–864, Oct. 1974.

[8] I. Wolff and V. K. Tripathi, "The microstrip open-ring resonator," *IEEE Trans. Microwave Theory Tech.*, vol. MTT-32, pp. 102–107, Jan. 1984.

[9] F. Giannini, R. Sorrentino, and J. Vrba, "Planar circuit analysis of microstrip radial stub," *IEEE Trans. Microwave Theory Tech.*, vol. MTT-32, pp. 1652–1655, Dec. 1984.

[10] K. C. Gupta and M. D. Abouzahra, "Analysis and design of four-port and five-port microstrip disc circuits," *IEEE Trans. Microwave Theory Tech.*, vol. MTT-33, pp. 1422–1428, Dec. 1985.

[11] W. K. Gwarek, "Analysis of an arbitrarily-shaped planar circuit—A time-domain approach," *IEEE Trans. Microwave Theory Tech.*, vol. MTT-33, pp. 1067–1072, Oct. 1985.

[12] P. Silvester, "Finite element analysis of planar microwave networks," *IEEE Trans. Microwave Theory Tech.*, vol. MTT-21, pp. 104–108, Feb. 1973.

[13] G. Conciauro, M. Bressan, and C. Zuffada, "Waveguide modes via an integral equation leading to a linear matrix eigenvalue problem," *IEEE Trans. Microwave Theory Tech.*, vol. MTT-32, pp. 1495–1504, Nov. 1984.

[14] P. Arcioni, M. Bressan, and G. Conciauro, "Wideband analysis of planar waveguide circuits," *Alta Frequenza*, June 1988.

[15] J. Van Bladel, *Electromagnetic Fields*. Washington: Hemisphere Publishing Corp , 1985.

[16] N. Marcuvitz, *Waveguide Handbook*. Cambridge MA: Radiation Lab. MIT, 1951.

[17] M. Bressan and G. Conciauro, "Singularity extraction from the electric Green's functions in two-dimensional resonators of circular or rectangular cross-section," *Alta Frequenza*, vol. LII, pp. 188–190, Mar. 1983.
[18] M. Bressan and G. Conciauro, "Singularity extraction from the electric Green's function for a spherical resonator," *IEEE Trans. Microwave Theory Tech.*, vol. MTT-33, pp. 407–414, May 1985.
[19] D. S. Jones, *Methods in Electromagnetic Wave Propagation*. Oxford: Clarendon Press, 1979.
[20] P. Arcioni and M. Bressan, "ANAPLAN: a package for the wide-band analysis of planar circuits," (in Italian) *Proc. Sesta Riunione Nazionale di Elettromagnetisimo Applicato* (Trieste), Oct. 22–24, 1986, pp. 305–308.
[21] J. N. Franklin, *Matrix Theory*. Englewood Cliffs, NJ: Prentice-Hall, 1968.

✠

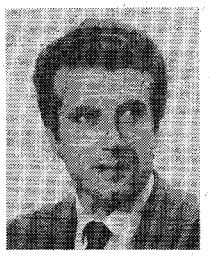

Paolo Arcioni was born in Busto Arsizio, Italy, in 1949. He received a degree in electronic engineering from the University of Pavia, Italy, in 1973.

After graduation, he joined the Department of Electronics of the University of Pavia as a researcher in electromagnetics. Since 1976 he has taught microwave theory as an Associate Professor at the University of Pavia. His main research interests concern the development of a numerical method for the electromagnetic CAD of microwave circuits.

Marco Bressan was born in Venice, Italy, in 1949. He graduated in electronic engineering at the University of Pavia, Italy, in 1972.

Since 1973 he has been with the Department of Electronics of the University of Pavia as a Researcher in the field of electromagnetics. Since 1987 he has taught on antennas and propagation as an Associate Professor at the University of Pavia. His main research interests involve analytical and numerical methods for studying microwave structures and inverse problems in electromagnetics.

✠

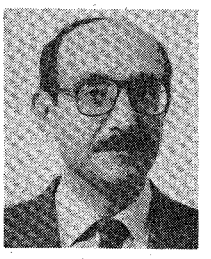

Giuseppe Conciauro (A'72–M'87) was born in Palermo, Italy, in 1937. He received the degree in electrical engineering from the University of Palermo, Italy, in 1961, and the "Libera Docenza" in electronics in 1971.

From 1963 to 1971 he was with the Istituto di Elettrotecnica of the University of Palermo as an Assistant Professor of microwave theory. In 1971 he joined the Department of Electronics of the University of Pavia, Italy, where he taught microwave theory as an Associate Professor. In 1980 he became Professor of electromagnetic theory. Presently, he is the Director of the Department of Electronics at the University of Pavia, where he teaches electromagnetic theory. His main research interests are in microwave theory, interaction structures for particle accelerators, and numerical methods in electromagnetics.

Prof. Conciauro is a member of AEI.